

Role of Entropy and Structural Parameters in the Spin State Transition of $LaCoO_3$

Bismayan Chakrabarti,¹ Turan Birol,^{1,2} and Kristjan Haule¹

¹*Department of Physics & Astronomy, Rutgers University, Piscataway, NJ 08854-8019, USA*

²*Department of Chemical Engineering and Materials Science,
University of Minnesota, Minneapolis, MN 55455-0132, USA*

(Dated: July 8, 2016)

The spin state transition in $LaCoO_3$ has eluded description for decades despite concerted theoretical and experimental effort. In this study, we approach this problem using charge consistent Density Functional Theory + Embedded Dynamical Mean Field Theory (DFT+DMFT). We show, from first principles, that $LaCoO_3$ cannot be described by a single, pure spin state at any temperature, but instead shows a gradual change in the population of higher spin multiples as temperature is increased. We explicitly elucidate the critical role of the lattice expansion and oxygen octahedral rotations in the spin state transition. We also show that the spin state transition and the metal-insulator transition in $LaCoO_3$ occur at different temperature scales. In addition, our results shed light on the importance of electronic entropy, which has so far been ignored in all first principles studies of this material.

The spin state transition in $LaCoO_3$ has been the subject of intensive investigation for decades.[1–3] This compound is established to be a narrow bandgap insulator at low temperature with Pauli-like magnetic susceptibility. However between 90-150 K, it transitions to a local moment phase with a Curie-Weiss like susceptibility which reaches its peak around 150K. It also undergoes a gradual closing of the insulating gap and is known to be metallic above 600K [4–6].

There is considerable debate regarding the mechanism of this transition, mainly due to the uncertainty regarding the multiplet of the Co^{3+} ion which characterizes the excited state of the compound. The cobalt ion in $LaCoO_3$ is commonly considered to have a formal valence of 3+ and to be in the d^6 state. The scale of the crystal field splitting is comparable to Hunds coupling energy scale. As a result, one would expect that as temperature is increased, there would be an entropy-driven transition from the low spin (LS) $S = 0$ state with a fully filled t_{2g} shell (t^6e^0) to an $S = 2$ high spin (HS) state (t^4e^2)[3]. Indeed there is experimental evidence that does support such a scenerio. Electron spin resonance[7], neutron scattering [8], X-ray absorbtion spectroscopy, and magnetic circular dichroism experiments[9] point towards a transition to an HS state. In addition, no inequivalent Co-O bond is found in EXAFS experiements, which also supports the formation of an HS state due to the HS state not being strongly Jahn-Teller active [10]. However, it has been noted that in order to explain the XAS experimental data, one would have to assume that the crystal field grows with temperature, which is counter-intuitive.[9, 11] This led to some authors suggesting that there is an LS-HS alternating structure caused by breathing distortions[12] [3] and interatomic repulsion between the HS atoms.[11, 13]

A competing explanation, whereby the excited state is the $S = 1$ intermediate spin (IS) state (t^5e^1), has also become popular[1, 14], mainly because of LDA+U results

which show that the IS state is lower in energy compared to the HS state.[15–17] The stability of the IS state has been justified by the large hybridization of the Co 3d electrons with neighboring O 2p electrons. This causes charge transfer between the ions resulting in the Co ion having a d^7 structure according to the Zaanen-Sawatzky-Allen scheme,[18] which in turn would cause stabilization of the IS state. The intermediate spin state hypothesis also seems to explain experimental findings such as Raman Spectroscopy, X-Ray photoemission, other XAS and EELS spectroscopies, as well as susceptibility and thermal expansion measurements. [6, 19–25].

To summarize, there has been a significant amount of debate regarding the true nature of the spin state transition in $LaCoO_3$. Interest in this compound has also been enhanced in light of recent discoveries of ferromagnetism induced by Sr (hole) doping [26–29], as well as experiments reporting strain induced magnetism in epitaxially grown thin films.[30? –35]. In addition, there have been reports of the emergence of a striped phase in thin films with alternating LS and HS/IS regions.[36] Low temperature ferromagnetism has also been reported in experiments on $LaCoO_3$ nanoparticles[37]. Hence, there is great interest in understanding the true behavior of this material.

In this letter, we use Density Functional Theory + embedded Dynamical Mean Field Theory (DFT+DMFT) to analyze spin state transition of bulk $LaCoO_3$. Our implementation extremizes the DFT+DMFT functional in real space, thereby avoiding the downfolding approximation and uses the numerically exact CTQMC impurity solver[3, 6]. Even though there are multiple recent studies that use DFT+DMFT on this compound [38–40], to our knowledge none of them provide a comprehensive analysis of all of the factors governing the transition such as octahedral rotations and electronic entropy. We show that i) $LaCoO_3$ has large charge fluctuations and it is not possible to explain the spin state with a single multiplet

at any temperature, ii) The crystal field splitting very sensitively depends on the details of the crystal structure, and taking into account not only the thermal expansion but also the oxygen octahedral rotations is very important, and iii) It is possible to stabilize an insulating phase (without orbital order) at intermediate temperatures where local moments are present, thereby showing that the metal-insulator transition is distinct from the spin state transition in this compound. We also show that iv) Electronic entropy difference between the high and low temperature states is necessary for the stabilization of the different spin states, which is a fact overlooked in various first principle studies so far.

Crystal Structure of LaCoO_3 — LaCoO_3 is a perovskite with space group $R\bar{3}c$ with significant oxygen octahedral rotations ($a^-a^-a^-$) and large thermal expansion. In order to investigate the effect of both of these structural parameters on the spin state transition, we not only use two different experimental structures for 4K and 1143K [41], but also create two cubic perovskite structures with the same inter-Lanthanum separation as the two experimental structures but with no oxygen octahedral rotations. We refer to these 4 structures as HTa^- , LTa^- , HTa^0 and LTa^0 with HT(high temperature) and LT(low temperature) denoting the temperature for the structural data, and a^- and a^0 denoting the presence and absence of rotations respectively.

In Fig 1 we show the density of states for all 4 structures, calculated at both low temperature and high temperature (116K and 1160K) using Density Functional Theory + Dynamical Mean Field Theory (DFT+DMFT).[45] Unlike DFT, which always predicts a metallic state, our calculations correctly reproduce an insulating ground state at low temperature for all the structures. The t_{2g} orbitals are below the fermi level whereas the e_g orbitals are above the fermi level.

The charge gap closes continuously with increasing temperature, and as a result, there is a large overlap in energy between the t_{2g} and e_g orbitals at high temperatures. This overlap, however, is much smaller if the structures without rotations are simulated. (See Fig. 2b).

The HTa^0 structure shows some overlap at high temperatures, and the LTa^0 structure almost remains an insulator for the entire range of temperature studied, with only a small overlap developing above 900K. This shows clearly that octahedral rotations play a large role in decreasing the strength of the crystal field splitting. This can be explained by a combination of factors. The rotation of the oxygen octahedra causes the misalignment of the crystal field of the O atoms with that of the La atoms, which normally reinforce each other in a perovskite with no octahedral rotations. This leads to an overall reduction of the effective crystal field which reduces the charge gap between the t_{2g} and the e_g orbitals. In addition, this trigonal distortion also leads to a splitting of the t_{2g} orbitals into 2+1 orbitals, thereby again reducing the

gap with the e_g orbitals. The combination of these two effects seems to overcome the expected decrease in the bandwidth of the e_g orbitals. Finally, note that there is a considerable overlap in energy of the O 2p orbitals with the Co 3d orbitals, which is very important in producing charge fluctuations on the Co ion, making it highly mixed-valent.

The spin state transition— In order to focus on the spin state of the Co ion, we calculate the expectation value of the magnitude of z-component of the spin $\langle |S_z| \rangle$. Note that all our calculations are in the paramagnetic state and hence the value of $\langle S_z \rangle = 0$. The results are presented in Fig. 2a as a function of temperature.[46] The largest value of $|S_z|$ at 1160K is seen for the HTa^- structure, followed by the LTa^- structure. This is in line with the stronger crystal field in the LTa^- structure due to the smaller lattice constant. We also observe that the spin state transition starts at a higher temperature for the LTa^- structure ($\sim 580\text{K}$) compared to the HTa^- ($\sim 380\text{K}$). This is also consistent with the low temperature structure having a higher stability for the LS state. The structures without rotations consistently show a lower buildup of higher spin states than the ones with rotations. The HTa^0 structure displays a spin state transition, but with an eventual high temperature value of $|S_z|$ that is lower. On the other hand, the LTa^0 structure shows almost no transition. This shows that the role that the octahedral rotations play in the reduction of the crystal field is essential for the spin state transition.

Figures 2a and 2b also show that the spin state transition and the charge gap closing occur at different temperatures, which is a trend that has been observed in experiment but has not been captured in earlier DMFT simulations. For example, Fig 2b shows that both the HTa^- and the LTa^- structures show a complete closure of the charge gap at $\sim 600\text{K}$ whereas Fig 2a shows that the spin state transition in the two structures occur at very different temperatures.

Nature of the excited spin state— Because of the large hybridization between Co and O, the d orbitals of Co have large charge fluctuations and all the four structures have an effective d-shell occupation of $n_d \sim 6.6$. Therefore any analysis of the spin states in terms of the LS, IS and HS states of the d^6 configuration of the Co ion is necessarily inadequate. In fact, our calculations show that the d^7 configuration has a higher occupation probability than d^6 , and there are also significant probabilities for d^5 and d^8 .

Fig. 3 shows the evolution of the occupation probabilities for the different values of $|S_z|$ with temperature. Even at high temperatures, $|S_z| = 0$ and $|S_z| = 0.5$ (the LS states for the even and odd occupancy sectors of the d orbital) remain the states with the highest probability. However, with the increase of temperature, the weight of the higher spin states increases. At the onset of the transition, the initial change in the value of the spin state is

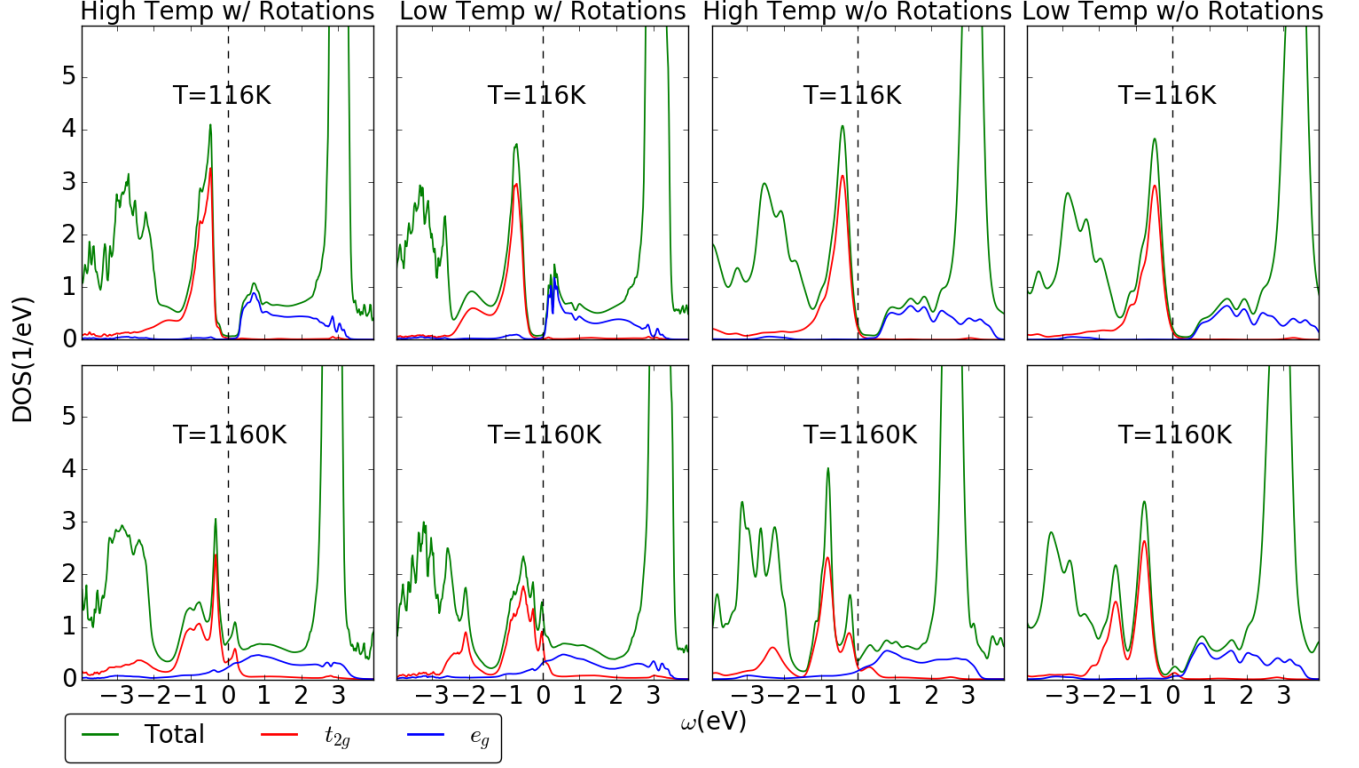


FIG. 1: Density of states (t_{2g} , e_g and total including all atoms) for all four structures at 116K and 1160K.

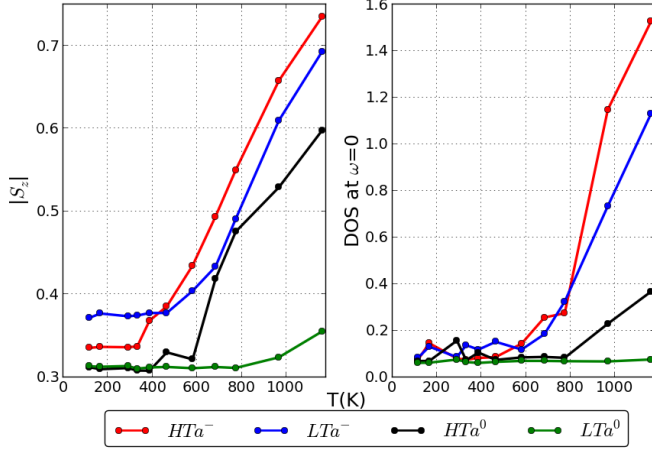


FIG. 2: (a) Evolution of $|S_z|$ with temperature for all four structures. (b) Evolution of Density of states at fermi level with temperature for all four structures.

predominantly caused by the excitation of the $|S_z| = 2$ and the $|S_z| = 1.5$ multiplets. The $|S_z| = 1$ multiplet sees an increase in probability at higher temperatures (above 500K) and also follows a similar trend for all the structures except the LTa^0 structure, where all changes are very small. Therefore, the initial signature of the transition is best seen in the behavior of the $|S_z| = 2.0$ and

$|S_z| = 1.5$ multiplets, which can be said to be the HS multiplets for the d^6 and d^7 occupancies respectively.

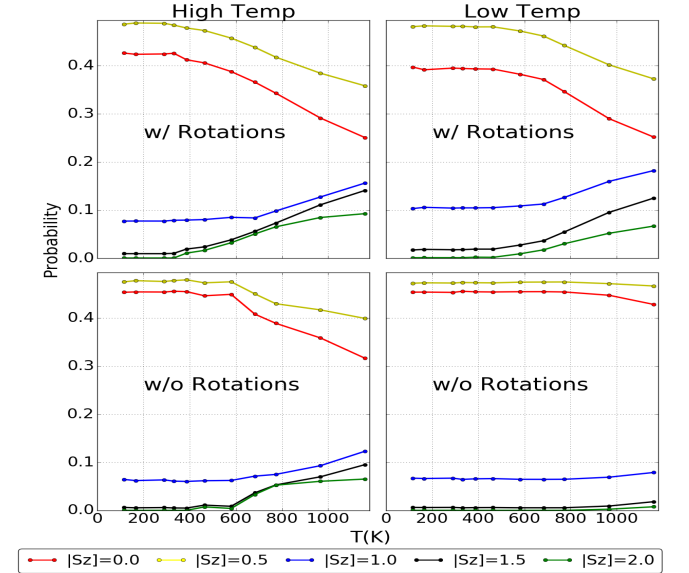


FIG. 3: Evolution of occupation probabilities for all the spin states for the four structures with temperature.

In Fig. 4, we show the occupancy histograms below and above the transition (at 116K and 1160K). (CTQMC

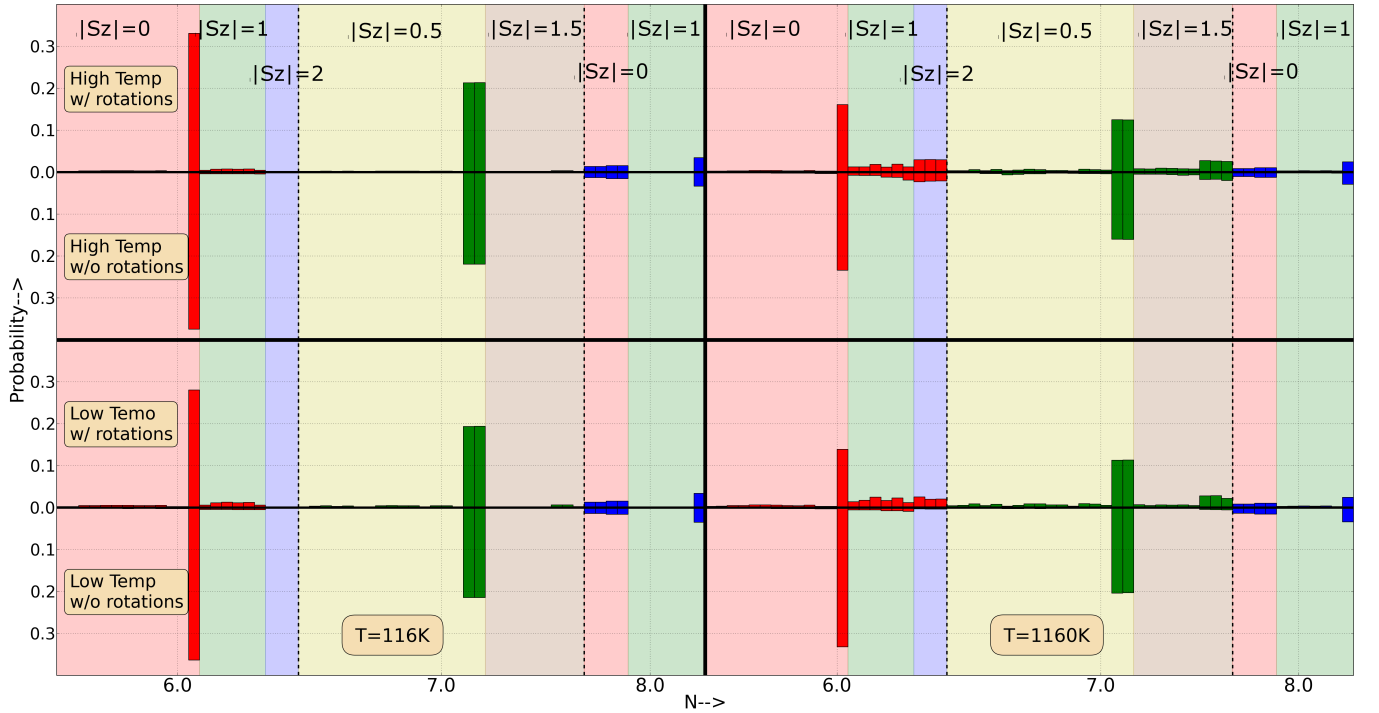


FIG. 4: Occupancy histogram showing the occupancy Probability for the different atomic states for the d orbital of the Co atom for all the four structures at two different temperatures. The different background colors mark the areas reserved for different spin sectors. The lower x axis ticks as well as the color of the histogram bars denote the different occupancies of the d orbital. Note that odd occupancies only allow half integer values of $|S_z|$ while even ones allow integer values

gives us access to the state space probability for each of the 1024 states of the d orbital. However, in order to aid visualization, we only show states which have an occupation probability above 0.001 in any of the structures at any temperature.) This figure displays clearly how the transition is marked by the excitation of states in the higher spin multiplets. We see that the low temperature state for all of the structures is marked by the presence of a few states with large probability (mainly corresponding to the $|S_z| = 0$ and $|S_z| = 0.5$ states). As the spin state transition sets in, a large number of higher spin states get excited and the LS spin states lose weight. Note that the high spin states are highly degenerate so there is no one large peak for the high spin states, but a multitude of lower peaks. This supports the idea that the transition is primarily an entropy driven transition. We can also get a good idea of the relative strengths of the transition for the different structures: The largest change occurs in the HTa^- structure, and the smallest one happens in the LTa^0 .

Contribution of Electronic Entropy— According to the entropy driven transition scenerio, which is supported by calorimetric measurements[43], LaCoO_3 favors higher spin multiplets at elevated temperatures because of the associated gain in electronic entropy as a result of the high degeneracy of these high spin states - a point missed by first principles calculations at the level of DFT. Access

to higher spin states is also made easier by a larger lattice constant due to the reduced crystal field, so the gain in electronic entropy could also be a driving factor for the large thermal expansion seen in this material.

We calculated the contribution of the electronic entropy to the free energy using our state of the art DFT+DMFT implementation[44]. In particular, we evaluated the Free Energy and the Electronic Entropy for both the 4K and 1143K structures (LTa^- and HTa^-) at 1160K to predict if the structural changes make a considerable difference. The HTa^- structure is indeed much higher in electronic entropy compared to the LTa^- structure at 1160K; the difference in $T \cdot S$ between these two structures is ~ 110 meV per formula unit. This unusually large difference emphasises the importance of electronic entropy to the transition. We also calculate the energy difference between the HTa^- and LTa^- structures to be ~ 70 meV at 1160K with the LTa^- being lower in energy. Thus we see that when the entropy is taken into account and the Free Energy ($F=E-TS$) is calculated, the high temperature structure HTa^- becomes more stable purely due to the contribution of electronic entropy. This result therefore confirms the structural phase transition that is observed as a function of temperature. So, we can conclude that the electronic entropy, which has been ignored in many first-principles studies of this material, is a leading factor in creating an anomalous thermal ex-

pansion and driving the material to a high spin state.

Summary— We studied the spin state transition of LaCoO_3 using state of the art fully charge self consistent DFT+DMFT. By using different experimental and hypothetical crystal structures, we disentangled the effect of different components of the crystal structure and showed that both the thermal expansion and the presence of oxygen octahedral rotations have tremendous effect on the spin state transition of LaCoO_3 . Our single site DMFT approach reproduced not only the spin state transition but also the intermediate phase which has nonzero magnetic moment but is insulating. This shows that the spin state and the metal-insulator transitions occur at different temperature scales and that the magnetic-insulating phase can be reproduced without necessarily involving cell doubling via mechanisms such as breathing distortions of spatially inhomogeneous mixed spin states. Our results emphasize the importance of charge fluctuations on the Co ion due to hybridization with the O anions, and thus point to the inadequacy of a simple spin state picture with only one formal valence. While the spin state transition is concurrent with a sudden change in occupation in the high spin multiplets, low and intermediate spin states also have significant occupation in the whole temperature range. Finally, our work is the first calculation of the electronic entropy of LaCoO_3 and it points to the fact that the difference of the contribution of entropy to the free energy is significant and is large enough to drive the spin state transition in this material.

Acknowledgements— TB was supported by the Rutgers Center for Materials Theory. BC and KH were supported by the NSF-DMR 1405303.

-
- [1] R. Heikes, R. Miller, and R. Mazelsky, *Physica* **30**, 1600 (1964), ISSN 0031-8914, URL <http://www.sciencedirect.com/science/article/pii/003189146490182X>.
 - [2] C. S. Naiman, R. Gilmore, B. DiBartolo, A. Linz, and R. Santoro, *Journal of Applied Physics* **36** (1965).
 - [3] P. M. Raccach and J. B. Goodenough, *Phys. Rev.* **155**, 932 (1967), URL <http://link.aps.org/doi/10.1103/PhysRev.155.932>.
 - [4] V. G. Bhide, D. S. Rajoria, G. R. Rao, and C. N. R. Rao, *Phys. Rev. B* **6**, 1021 (1972), URL <http://link.aps.org/doi/10.1103/PhysRevB.6.1021>.
 - [5] S. R. English, J. Wu, and C. Leighton, *Phys. Rev. B* **65**, 220407 (2002), URL <http://link.aps.org/doi/10.1103/PhysRevB.65.220407>.
 - [6] T. Saitoh, T. Mizokawa, A. Fujimori, M. Abbate, Y. Takeda, and M. Takano, *Phys. Rev. B* **55**, 4257 (1997), URL <http://link.aps.org/doi/10.1103/PhysRevB.55.4257>.
 - [7] Z. Ropka and R. J. Radwanski, *Phys. Rev. B* **67**, 172401 (2003), URL <http://link.aps.org/doi/10.1103/PhysRevB.67.172401>.
 - [8] A. Podlesnyak, S. Streule, J. Mesot, M. Medarde, E. Pomjakushina, K. Conder, A. Tanaka, M. W. Haverkort, and D. I. Khomskii, *Phys. Rev. Lett.* **97**, 247208 (2006), URL <http://link.aps.org/doi/10.1103/PhysRevLett.97.247208>.
 - [9] M. W. Haverkort, Z. Hu, J. C. Cezar, T. Burnus, H. Hartmann, M. Reuther, C. Zobel, T. Lorenz, A. Tanaka, N. B. Brookes, et al., *Phys. Rev. Lett.* **97**, 176405 (2006), URL <http://link.aps.org/doi/10.1103/PhysRevLett.97.176405>.
 - [10] N. Sundaram, Y. Jiang, I. E. Anderson, D. P. Belanger, C. H. Booth, F. Bridges, J. F. Mitchell, T. Profen, and H. Zheng, *Phys. Rev. Lett.* **102**, 026401 (2009), URL <http://link.aps.org/doi/10.1103/PhysRevLett.102.026401>.
 - [11] R. Eder, *Phys. Rev. B* **81**, 035101 (2010), URL <http://link.aps.org/doi/10.1103/PhysRevB.81.035101>.
 - [12] R. A. Bari and J. Sivardi re, *Phys. Rev. B* **5**, 4466 (1972), URL <http://link.aps.org/doi/10.1103/PhysRevB.5.4466>.
 - [13] T. Ky men, Y. Asaka, and M. Itoh, *Phys. Rev. B* **71**, 024418 (2005), URL <http://link.aps.org/doi/10.1103/PhysRevB.71.024418>.
 - [14] P. G. Radaelli and S.-W. Cheong, *Phys. Rev. B* **66**, 094408 (2002), URL <http://link.aps.org/doi/10.1103/PhysRevB.66.094408>.
 - [15] M. A. Korotin, S. Y. Ezhov, I. V. Solovyev, V. I. Anisimov, D. I. Khomskii, and G. A. Sawatzky, *Phys. Rev. B* **54**, 5309 (1996), URL <http://link.aps.org/doi/10.1103/PhysRevB.54.5309>.
 - [16] S. K. Pandey, A. Kumar, S. Patil, V. R. R. Medicherla, R. S. Singh, K. Maiti, D. Prabhakaran, A. T. Boothroyd, and A. V. Pimpale, *Phys. Rev. B* **77**, 045123 (2008), URL <http://link.aps.org/doi/10.1103/PhysRevB.77.045123>.
 - [17] I. A. Nekrasov, S. V. Streltsov, M. A. Korotin, and V. I. Anisimov, *Phys. Rev. B* **68**, 235113 (2003), URL <http://link.aps.org/doi/10.1103/PhysRevB.68.235113>.
 - [18] J. Zaanen, G. A. Sawatzky, and J. W. Allen, *Phys. Rev. Lett.* **55**, 418 (1985), URL <http://link.aps.org/doi/10.1103/PhysRevLett.55.418>.
 - [19] M. Abbate, J. C. Fuggle, A. Fujimori, L. H. Tjeng, C. T. Chen, R. Potze, G. A. Sawatzky, H. Eisaki, and S. Uchida, *Phys. Rev. B* **47**, 16124 (1993), URL <http://link.aps.org/doi/10.1103/PhysRevB.47.16124>.
 - [20] S. Masuda, M. Aoki, Y. Harada, H. Hirohashi, Y. Watanabe, Y. Sakisaka, and H. Kato, *Phys. Rev. Lett.* **71**, 4214 (1993), URL <http://link.aps.org/doi/10.1103/PhysRevLett.71.4214>.
 - [21] R. F. Klie, J. C. Zheng, Y. Zhu, M. Varela, J. Wu, and C. Leighton, *Phys. Rev. Lett.* **99**, 047203 (2007), URL <http://link.aps.org/doi/10.1103/PhysRevLett.99.047203>.
 - [22] C. Zobel, M. Kriener, D. Bruns, J. Baier, M. Gr ninger, T. Lorenz, P. Reutler, and A. Revcolevschi, *Phys. Rev. B* **66**, 020402 (2002), URL <http://link.aps.org/doi/10.1103/PhysRevB.66.020402>.
 - [23] V. Gnezdilov, V. Fomin, A. V. Yermenko, K.-Y. Choi, Y. Pashkevich, P. Lemmens, S. Shiryayev, G. Bychkov, and S. Barilo, *Low Temperature Physics* **32** (2006).
 - [24] G. Maris, Y. Ren, V. Volotchaev, C. Zobel, T. Lorenz, and T. T. M. Palstra, *Phys. Rev. B* **67**, 224423 (2003), URL <http://link.aps.org/doi/10.1103/PhysRevB.67.224423>.
 - [25] T. Vogt, J. A. Hriljac, N. C. Hyatt, and P. Woodward,

- Phys. Rev. B **67**, 140401 (2003), URL <http://link.aps.org/doi/10.1103/PhysRevB.67.140401>.
- [26] M. Kriener, C. Zobel, A. Reichl, J. Baier, M. Cwik, K. Berggold, H. Kierspel, O. Zabara, A. Freimuth, and T. Lorenz, Phys. Rev. B **69**, 094417 (2004), URL <http://link.aps.org/doi/10.1103/PhysRevB.69.094417>.
- [27] M. Itoh, I. Natori, S. Kubota, and K. Motoya, Journal of the Physical Society of Japan **63**, 1486 (1994), <http://dx.doi.org/10.1143/JPSJ.63.1486>, URL <http://dx.doi.org/10.1143/JPSJ.63.1486>.
- [28] P. Augustinský, V. Krápek, and J. Kuneš, Phys. Rev. Lett. **110**, 267204 (2013), URL <http://link.aps.org/doi/10.1103/PhysRevLett.110.267204>.
- [29] Z. Németh, A. Szabó, K. Knížek, M. Sikora, R. Chernikov, N. Sas, C. Bogdán, D. L. Nagy, and G. Vankó, Phys. Rev. B **88**, 035125 (2013), URL <http://link.aps.org/doi/10.1103/PhysRevB.88.035125>.
- [30] D. Fuchs, C. Pinta, T. Schwarz, P. Schweiss, P. Nagel, S. Schuppler, R. Schneider, M. Merz, G. Roth, and H. v. Löhneysen, Phys. Rev. B **75**, 144402 (2007), URL <http://link.aps.org/doi/10.1103/PhysRevB.75.144402>.
- [31] D. Fuchs, E. Arac, C. Pinta, S. Schuppler, R. Schneider, and H. v. Löhneysen, Phys. Rev. B **77**, 014434 (2008), URL <http://link.aps.org/doi/10.1103/PhysRevB.77.014434>.
- [32] J. M. Rondinelli and N. A. Spaldin, Phys. Rev. B **79**, 054409 (2009), URL <http://link.aps.org/doi/10.1103/PhysRevB.79.054409>.
- [33] J. W. Freeland, J. X. Ma, and J. Shi, Applied Physics Letters **94**, 129903 (2009), URL <http://scitation.aip.org/content/aip/journal/apl/94/12/10.1063/1.3097551>.
- [34] D. Fuchs, L. Dieterle, E. Arac, R. Eder, P. Adelman, V. Eyert, T. Kopp, R. Schneider, D. Gerthsen, and H. v. Löhneysen, Phys. Rev. B **79**, 024424 (2009), URL <http://link.aps.org/doi/10.1103/PhysRevB.79.024424>.
- [35] A. Herklotz, A. D. Rata, L. Schultz, and K. Dörr, Phys. Rev. B **79**, 092409 (2009), URL <http://link.aps.org/doi/10.1103/PhysRevB.79.092409>.
- [36] W. S. Choi, J.-H. Kwon, H. Jeon, J. E. Hamann-Borrero, A. Radi, S. Macke, R. Sutarto, F. He, G. A. Sawatzky, V. Hinkov, et al., Nano Letters **12**, 4966 (2012), pMID: 22889011, <http://dx.doi.org/10.1021/nl302562f>, URL <http://dx.doi.org/10.1021/nl302562f>.
- [37] A. M. Durand, D. P. Belanger, T. J. Hamil, F. Ye, S. Chi, J. A. Fernandez-Baca, C. H. Booth, Y. Abdollahian, and M. Bhat, Journal of Physics: Condensed Matter **27**, 176003 (2015), URL <http://stacks.iop.org/0953-8984/27/i=17/a=176003>.
- [38] L. Craco and E. Müller-Hartmann, Phys. Rev. B **77**, 045130 (2008), URL <http://link.aps.org/doi/10.1103/PhysRevB.77.045130>.
- [39] G. Zhang, E. Gorelov, E. Koch, and E. Pavarini, Phys. Rev. B **86**, 184413 (2012), URL <http://link.aps.org/doi/10.1103/PhysRevB.86.184413>.
- [40] V. Krápek, P. Novák, J. Kuneš, D. Novoselov, D. M. Korotin, and V. I. Anisimov, Phys. Rev. B **86**, 195104 (2012), URL <http://link.aps.org/doi/10.1103/PhysRevB.86.195104>.
- [41] G. Thornton, B. Tofield, and A. Hewat (1986).
- [42] See the supplemental information..
- [43] S. Stølen, F. Grønvald, H. Brinks, T. Atake, and H. Mori, Phys. Rev. B **55**, 14103 (1997), URL <http://link.aps.org/doi/10.1103/PhysRevB.55.14103>.
- [44] K. Haule and T. Birol, Phys. Rev. Lett. **115**, 256402 (2015), URL <http://link.aps.org/doi/10.1103/PhysRevLett.115.256402>.
- [45] The details of the calculations are presented in the supplemental information.
- [46] Note that the quantitative value of the transition temperature is overestimated in our calculations. This can be explained by the fact that DMFT does not take into account finite wavelength fluctuations, and as a result, has a tendency to overestimate order like many other mean field methods.

**Supplementary Material for
“Role of Entropy and Structural Parameters in the Spin State Transition of LaCoO_3 ”**

DETAILS OF THE CRYSTAL STRUCTURE

LaCoO_3 is a perovskite, which has the rare earth La on the A-site and Co on the B-site, which corresponds to the center of the oxygen octahedron. However, like most of the perovskites, LaCoO_3 has oxygen octahedral rotations (Fig. S1) which involve the oxygen octahedra rotating out-of-phase around the $[111]$ axes of the undistorted cubic highsymmetry structure. The rotation pattern in Glazer notation is $a^-a^-a^-$, which corresponds to the space group $R\bar{3}c$ (#167).

As noted by Thornton et. al. [S1], LaCoO_3 has large thermal expansion and the octahedral rotation angle also changes with temperature. In our study, we used four different crystal structures to isolate and study the effect of different lattice parameters on the spin state transition. We used the two different experimental structures observed at 1143K and 4K, which we denote by HTa^- and LTa^- . Comparing the electronic structure for these two crystal structures provides a means to study the temperature evolution of the electronic structure. In addition to these two, we also built two cubic perovskite crystal structures with the same inter-Lanthanum spacing as them, but with no octahedral rotations. These structures, denoted by HTa^0 and LTa^0 , enabled us to isolate the effect of oxygen octahedral rotations on the electronic structure of LaCoO_3 .

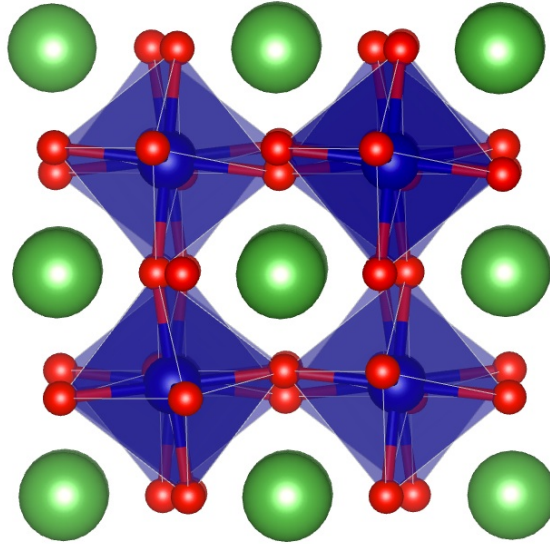


FIG. S1: A depiction of the pattern of octahedral rotations that is present in LaCoO_3 . Each of the oxygen octahedra rotates in the opposite direction to all nearest neighbour octahedra by the same amount relative to all three coordinate axes ($a^-a^-a^-$ structure).

DETAILS OF THE DFT+DMFT CALCULATIONS

We performed fully charge self-consistent embedded DFT+DMFT calculations[S2][S3][S4] on LaCoO_3 . Our implementation is based on the Wien2K all-electron DFT package.[S5] For the DFT functional we use the GGA-PBE functional. We employed a 10 atom unit cell for the 2 structures with rotations and 5 atom unit cells for the two structures without rotations and used 512 k points in the first Brillouin zone. Our DMFT implementation uses state-of-the-art CTQMC[S6] impurity solver based on the hybridization expansion (CTQMC-HYB) and all simulations are iterated to self-consistency. It is to be noted that our implementation makes use of projectors to embed/project out the impurity self-energy onto the lattice degrees of freedom. This prevents errors associated with downfolding using Wannier orbitals and allows us to achieve highly accurate charge self-consistency.[S3] We also account for octahedral

rotations, wherever present, by applying local rotations so as to align our correlated orbitals with the local crystal field set up by the neighboring atoms. In our simulations, we use a Hubbard U of 6.0 eV and Hund's coupling (J) of 0.7eV. We have also investigated the effects of varying the value of J , and found that this does not change the temperature at which the transitions occur, but merely changes the value of the observed $|S_z|$ by a small amount, with higher J values resulting in slightly larger values. We ignored the spin-orbit interaction, as it is expected to be small in this 3d transition metal oxide.

The typical self-consistent calculation requires 30 self consistency cycles each with around 10 DFT iterations and one CTQMC iteration per cycle. Our LDA+DMFT calculations gave us the Green's function ($G(i\omega)$) on the imaginary (Matsubara) axis which we analytically continued using the maximum entropy method to get the density of states on the real axis.

TECHNICAL DETAILS OF OUR DFT+DMFT FRAMEWORK

DMFT is based on mapping the original lattice problem to an auxilliary impurity problem . We minimize the action of this impurity problem defined by:

$$\mathcal{S} = \int_0^\beta d\tau \psi_{L\sigma}^\dagger(\tau) \frac{\partial}{\partial \tau} \psi_{L\sigma}(\tau) + \int_0^\beta d\tau \int_0^\beta d\tau' \psi^\dagger(\tau') \Delta_{L_1\sigma, L_2\sigma'} \psi(\tau) \\ + \frac{1}{2} \int_0^\beta d\tau \sum_{L_1, L_2, L_3, L_4, \sigma, \sigma'} U_{L_1, L_2, L_3, L_4} \psi_{L_1\sigma}^\dagger(\tau) \psi_{L_2\sigma'}^\dagger(\tau) \psi_{L_3\sigma'}(\tau) \psi_{L_4\sigma}(\tau) \quad (\text{S1})$$

where τ is imaginary time, L and σ denote angular momentum and spin labels, ψ and ψ^\dagger are the annihilation and creation operators for impurity electrons, Δ is the hybridization function between our impurity and the bath, which encodes most of the lattice information. The on-site Coulomb repulsion between the Co d-electrons is given by

$$\hat{U} = \frac{1}{2} \sum_{L_1, L_2, L_3, L_4, \sigma, \sigma'} U_{L_1, L_2, L_3, L_4} c_{L_1\sigma}^\dagger c_{L_2\sigma'}^\dagger c_{L_3\sigma'} c_{L_4\sigma} \quad (\text{S2})$$

where

$$U_{L_1, L_2, L_3, L_4} = \sum_k \frac{4\pi}{2k+1} \langle Y_{L_1} | Y_{km} | Y_{L_4} \rangle \langle Y_{L_2} | Y_{km}^* | Y_{L_3} \rangle F_{l_1, l_2, l_3, l_4}^k \quad (\text{S3})$$

where Y denotes spherical harmonics and F^k denote Slater integrals. The CTQMC impurity solver gives us the impurity self-energy Σ . Since correlations are very local in real space, we embed this self-energy by expanding it in terms of quasi-localized atomic orbitals, $|\phi_n^m\rangle$;

$$\Sigma_{i\omega}(r, r') = \sum_{mm', nn'} \langle r | \phi_n^m \rangle \langle \phi_n^m | \Sigma | \phi_{n'}^{m'} \rangle \langle \phi_{n'}^{m'} | r' \rangle \quad (\text{S4})$$

where m, m' denote the sites of Co atoms in the most general cluster-DMFT implementation and n, n' denote the atomic degrees of freedom for each site. Since, we perform single site DMFT, $\sum_{mm'}$ becomes $\delta_{m, m'}$. We then solve the Dyson equation in real space (or an equivalent complete basis such as the Kohn-Sham basis) according to the equation:

$$G_{i\omega}(r, r') = ((i\omega + \mu + \nabla^2 + V_{KS}(r)) \delta(r - r') - \Sigma_{i\omega}(r, r')) \quad (\text{S5})$$

This procedure is what we define as embedded DMFT, because the self energy is embedded into a large Hilbert Space instead of constructing a Hubbard-like model by downfolding to a few bands using Wannier Orbitals. This method has the advantage that the correlations are much more localized in real space compared to the Wannier representation, which makes DMFT a much better approximation. In addition, this formulation of DFT+DMFT can be shown to be derivable from the Luttinger Ward Functional which makes the formulation stationary and conserving [S7].

COMMENT ON FIGURE 2B

While calculating the density of states(DOS) at $\omega = 0$ for the different structures at different temperatures, we ensured that their Fermi energies were adjusted such that the energy levels for the oxygen densities of states lay at the same energy values. This was required because there was an ambiguity in the value of the chemical potential at temperatures where the structure gave rise to an insulating band-gap and we believe an accurate comparison can only be made if some features of the DOS are held fixed. This procedure required a shift in the chemical potential of some of the simulations of the order of 0.1 eV. The results we plot in Fig 2b are obtained after these shifts are put in. Figure 1 on the other hand plots the densities of states before any such post-processing has been done. This leads to small differences between the two figures. Instead of fixing the Oxygen levels, we also tried fixing the Lanthanum f levels and this gave rise to very similar results. We firmly believe that our results displayed in figure 2b are robust and it is merely the relevant magnitudes of the y-axis values at high temperatures that fluctuate by a small amount (depending on which features are held fixed) and not the actual temperature at which the charge-gap closure takes place. We also do not plot the DOS at $\omega = 0$ but the average of the DOS at five points around $\omega = 0$ as this takes care of some of the numerical noise that creeps into our calculation due to both Monte Carlo noise and the errors in analytic continuation. We also tested our results by averaging over different number of points and no significant changes take place that would affect our claims.

-
- [S1] G. Thornton, B. Tofield, and A. Hewat, Journal of Solid State Chemistry **61**, 301 (1986).
 - [S2] A. Georges, G. Kotliar, W. Krauth, and M. J. Rozenberg, Rev. Mod. Phys. **68**, 13 (1996), URL <http://link.aps.org/doi/10.1103/RevModPhys.68.13>.
 - [S3] K. Haule, C.-H. Yee, and K. Kim, Phys. Rev. B **81**, 195107 (2010), URL <http://link.aps.org/doi/10.1103/PhysRevB.81.195107>.
 - [S4] G. Kotliar, S. Y. Savrasov, K. Haule, V. S. Oudovenko, O. Parcollet, and C. A. Marianetti, Rev. Mod. Phys. **78**, 865 (2006), URL <http://link.aps.org/doi/10.1103/RevModPhys.78.865>.
 - [S5] P. Blaha, K. Schwarz, G. K. H. Madsen, D. Kvasnicka, and J. Luitz, *WIEN2K, An Augmented Plane Wave + Local Orbitals Program for Calculating Crystal Properties* (Karlheinz Schwarz, Techn. Universität Wien, Austria, 2001).
 - [S6] K. Haule, Phys. Rev. B **75**, 155113 (2007), URL <http://link.aps.org/doi/10.1103/PhysRevB.75.155113>.
 - [S7] K. Haule and T. Birol, Phys. Rev. Lett. **115**, 256402 (2015), URL <http://link.aps.org/doi/10.1103/PhysRevLett.115.256402>.